V during 1 min of operation. The current versus time curve showed a rapidly decaying current upon voltage switching, indicating the fast nature of the redox process for the device. Fig. 4D reveals that the total change in transmission from the bleached to the colored state consumed 0.5 mC of charge in 1 s. Within the first 100 ms, there was a fast coloration change with a 21% increase in transmittance, and 68% of total charge was consumed (as compared with the charge consumed after 1 s). This speed is comparable to good inorganic-based EC displays (*39*).

Conclusions. Our findings are significant for the area of electrochemical devices based on π-conjugated polymers because they can lead to long periods of stable device performance. This phenomenon was demonstrated for polyaniline fiber and yarn actuators, polypyrrole tube actuators, and for simple π-conjugated polymer electrochromic windows and numeric displays. The use of environmentally stable, room-temperature ionic liquids as electrolyte systems should have an impact on many areas of application in π-conjugated polymer electrochemical devices. Furthermore, as demonstrated herein for different π-conjugated polymer thin films, improved synthesis from ionic liquids may have positive effects on both their structure and properties.

References and Notes

1. T. A. Skotheim, R. L. Elsenbaumer, J. R. Reynolds, Eds., *Handbook of Conducting Polymers* (Dekker, New York, 1998).
2. W. Lu, B. R. Mattes, A. G. Fadeev, U.S. and PCT Patent Applications, filed on 21 December 2001.
3. W. Takashima, M. Kaneko, K. Kaneto, A. G. MacDiarmid, *Synth. Met.* **71**, 2265 (1995).
4. E. Smela, O. Inganäs, I. Lundström, *Science* **268**, 1735 (1995).
5. R. H. Baughman, *Synth. Met.* **78**, 339 (1996).
6. T. W. Lewis, S. E. Moulton, G. M. Spinks, G. G. Wallace, *Synth. Met.* **85**, 1419 (1997).
7. A. Della Santa, D. De Rossi, A. Mazzoldi, *Synth. Met.* **90**, 93 (1997).
8. Q. Pei, O. Inganäs, *Sol. State Ion.* **60**, 161 (1993).
9. M. R. Gandhi, P. Murray, G. M. Spinks, G. G. Wallace, *Synth. Met.* **73**, 247 (1995).
10. L. Bay, T. Jacobsen, S. Skaarup, K. West, *J. Phys. Chem. B* **105** (36), 8492 (2001).
11. T. Kobayashi, H. Yoneyama, H. Tamura, *J. Electroanal. Chem.* **161** (1984).
12. E. M. Genies, C. Tsintavis, *J. Electroanal. Chem.* **200**, 127 (1986).
13. Y. Li, R. Qian, *Synth. Met.* **53**, 149 (1993).
14. A. Mazzoldi, C. Degl'Innocenti, M. Michelucci, D. De Rossi, *Mater. Sci. Eng.* **C6**, 65 (1998).
15. W. Lu, B. R. Mattes, in preparation
16. T. W. Lewis, G. M. Spinks, G. G. Wallace, D. De Rossi, M. Pachetti, *Polym. Prep.* **38**, 520 (1997).
17. P. Walden, *Bull. Acad. Imper. Sci.* (St. Petersburg), 1800 (1914).
18. M. Freemantle, *Chem. Eng. News.* **78**, 37 (2000).
19. D. R. MacFarlane, M. Forsyth, *Adv. Mater.* **13**, 957 (2001).
20. C. Tiyapiboonchaiya, D. R. MacFarlane, J. Sun, M. Forsyth, *Macromol. Chem. Phys.*, in press.
21. V. R. Koch, C. Nanjundiah, G. B. Appetecchi, B. Scrosati, *J. Electrochem. Soc.* **142**, L116 (1995).
22. J. S. Wilkes, M. J. Zaworotko, *Chem. Commun.* **1992**, 965 (1992).
23. R. T. Carlin, H. C. D. Long, J. Fuller, P. C. Trulove, *J. Electrochem. Soc.* **141**, L73 (1994).
24. P. Bonhôte, A.-P. Dias, N. Papageorgiou, K. Kalyanasundaram, M. Grätzel, *Inorg. Chem.* **35**, 1168 (1996).
25. N. Papageorgiou *et al.*, *J. Electrochem. Soc.* **143**, 3099 (1996).
26. J. Tang, R. A. Osteryoung, *Synth. Met.* **45**, 1 (1991).
27. ———, *Synth. Met.* **44**, 307 (1991).
28. Materials and methods are available as supporting material at *Science* Online.
29. J. E. Huber, N. A. Fleck, M. F. Ashby, *Proc. R. Soc. Lond. A* **453**, 2185 (1997).
30. J. D. Madden, R. A. Cush, T. S. Kanigan, I. W. Hunter, *Synth. Met.* **113**, 185 (2000).
31. An asymmetric square wave pulse (40 s for oxidation and 30 s for reduction) allows the fiber to achieve steady states of actuation and balanced motion in the experiment.
32. T. F. Otero, J. M. Sansiñena, *Bioelectrochem. Bioenerg.* **42**, 117 (1997).
33. J. B. Schlenoff, H. Xu, *J. Electrochem. Soc.* **9**, 2397 (1992).
34. F. Beck, U. Barsch, R. Michaelis, *J. Electroanal. Chem.* **351**, 169 (1993).
35. It has come to our attention since acceptance of this paper that cycling [BMIM][PF_6] at potentials beyond its electrochemical window may lead to decomposition products that form an explosive mix. Caution from the authors is thus advised in selecting appropriate potential limits.
36. P. Chandrasekhar *et al.*, *Adv. Funct. Mater.* **12**, 95 (2002).
37. D. DeLongchamp, P. T. Hammond, *Adv. Mater.* **13**, 1455 (2001).
38. S. A. Sapp, G. A. Sotzing, J. R. Reynolds, *Chem. Mater.* **10**, 2101 (1998).
39. M. Gratzel, *Nature* **409**, 575 (2001).

40. The polyaniline fiber actuator and the electrochromic devices in [BMIM][BF_4] material are based on work supported by the Defense Advanced Research Projects Agency Defense Sciences Office for which the Santa Fe authors are thankful. The Australian Research Council and Quantum Technology of Sydney supported the polypyrrole tube in [BMIM][PF_6] actuator work for which the Wollongong and Monash University contributors are grateful.

Supporting Online Material

www.sciencemag.org/cgi/content/full/1072651/DC1
Materials and Methods
Figs. S1 to S7
Movies S1 and S2

8 April 2002; accepted 20 June 2002
Published online 4 July 2002;
10.1126/science.1072651
Include this information when citing this paper.

Brownian Motion of DNA Confined Within a Two-Dimensional Array

Dmytro Nykypanchuk, Helmut H. Strey,* David A. Hoagland*

Linear DNA molecules are visualized while undergoing Brownian motion inside media patterned with molecular-sized spatial constraints. The media, prepared by colloidal templating, trap the macromolecules within a two-dimensional array of spherical cavities interconnected by circular holes. Across a broad DNA size range, diffusion does not proceed by the familiar mechanisms of reptation or sieving. Rather, because of their inherent flexibility, DNA molecules strongly localize in cavities and only sporadically "jump" through holes. Jumping closely follows Poisson statistics. By reducing DNA's configurational freedom, the holes act as molecular weight–dependent entropic barriers. Sterically constrained macromolecular diffusion underlies many separation methods and assumes an important role in intracellular and extracellular transport.

Under incessant Brownian motion, mobile macromolecules in gels, membranes, or cytoplasm constantly squeeze through and around molecular-size obstructions. Until recently, neither the surroundings nor the motion of a single molecule could be directly observed, and the understanding of such sterically constrained motions was principally deduced through examination of the macroscopic diffusion coefficient. The dynamics of a single, large macromolecule can now be visually monitored by fluorescence microscopy (*1–4*), but studies of macromolecular diffusion by this approach have not extended to environments providing well-defined spatial constraints. We describe how to prepare highly ordered media in which macromolecular motion can be observed. Our preparation method, colloidal templating, provides regular microporous arrays of controlled geometry and chemistry.

Three basic mechanisms have emerged to explain how flexible macromolecules diffuse within a constraining medium—sieving, en-

Department of Polymer Science and Engineering, University of Massachusetts Amherst, Amherst, MA 01003, USA.

*To whom correspondence should be addressed. E-mail: strey@mail.pse.umass.edu (H.H.S.) and dah@neurotica.pse.umass.edu (D.A.H.).

tropic barriers transport, and reptation (*5*, *6*). The first of these treats each macromolecule as a rigid sphere, assigning a fixed radius equal to the molecule's average size. The medium's smaller pores and constrictions block passage, so with fewer traversable pathways, a larger molecule diffuses more slowly than a smaller one (*7*). Entropic barriers transport applies when the configuration of a flexible macromolecule must deform or fluctuate to pass through a medium's spatial constraints. At each position, the number of accessible configurations defines the molecule's local entropy. Entropy differences derived from the medium's spatial heterogeneity drive molecules to partition or localize preferentially in less constrictive spaces, where their enhanced configurational freedom raises entropy (*8*). Diffusion then occurs by thermally activated jumps across the intervening entropic barriers (*9*–*11*). Reptation can be envisioned as imposing lateral confinement on a diffusing linear macromolecule by enveloping the molecule in a fictitious tube. Only end segments can escape as the molecule undergoes random curvilinear motion along the tube axis (*12*–*14*). The tube's random contour and the molecule's sliding friction combine to hinder center-of-mass displacement. In contrast to entropic barriers transport, the number of configurations accessible to a reptating macromolecule does not depend on position. Which diffusion mechanism prevails under given conditions remains an open question (*15*, *16*). Sequential transitions from sieving to entropic barriers transport to reptation have been postulated as molecular weight or confinement increases (*5*, *6*). Such transitions, however, may not always be distinct.

By infusion and subsequent polymerization of a liquid monomer, colloidal templating replicates in a polymeric solid the structure of a precursor colloidal array (*17*–*19*). For this study, the precursor array consists of nearly monodisperse polystyrene spheres (0.895 μm in diameter) deposited from water and ethanol mixtures on a flat substrate (glass) to form a two-dimensional, hexagonally packed monolayer. The monomer (30% acrylamide and bisacrylamide in water) is introduced as an overcoating solution that polymerizes and cross-links to form a dense, transparent hydrogel film. Detachment of the substrate reveals a film surface decorated with an exposed area (~0.10 μm in radius) for each embedded sphere. These areas facilitate dissolution of the spheres when the film is immersed in an appropriate solvent (toluene). Left behind by dissolution is a close-packed array of cavities (0.92 μm in diameter, after equilibration with buffer), each connected to its six nearest neighbors by small round holes (0.10 μm in radius). A small perpendicular electric field induces DNA molecules in a fluorescent dye–containing buffer [1× TAE (x40 mm tris-acetate, 1 mm EDTA, pH 8.0) containing 5 mM sodium ascorbate and 10 mM NaCl] to enter the cavity array via the openings created during sphere dissolution. The dye (TOTO-1, Molecular Probes, Eugene, Oregon) is mixed with DNA at a ratio of 1 dye molecule to 6 base pairs; at this ratio, dye intercalation extends DNA length by about 33% (*20*). After sealing the exterior film openings with silicone oil, one can image the array and its trapped DNA by a combination of transmission and fluorescence microscopy. As shown in Fig. 1, the DNA molecules can freely explore the cavity array but are too large to penetrate the surrounding gel matrix.

Figure 2A superimposes transmission and fluorescence still frames of four neighboring 7.25–kilobase pair (kbp) DNA fragments of a 3.4-μm contour length and a 0.26-μm equilibrium (unconfined) radius of gyration. Figure 2B overlays 500 subsequent exposures of 0.5 s; over the 250-s time period, molecules variously moved through eight to 14 cavities. A closer look at the path followed by one molecule is provided in Fig. 2C. As suggested by the figure and easily discerned in the associated movie [see Movie S1 in the supporting online material (SOM)], diffusion occurs via discrete jumps from cavity to cavity, with rapid jumps (<1 s), separated by long periods (with an 18-s average) over which molecules remain essentially stationary. Even with centers of mass localized inside single cavities, small chain sections continuously probe neighboring cavities. Details of the probing are hard to resolve, but growth of a probing fluctuation beyond a threshold extension likely leads to an abrupt jump of an entire molecule. Molecules are rarely observed to straddle adjacent cavities, and when they do, they slip into one of the cavities by the next frame. The color code and jumping times attached to Fig. 2C reveal how the highlighted molecule jumped through the array. Extended illumination in the microscope causes a small fraction of molecules to degrade, and this fraction, along with any molecules that approached lattice defects, is discarded from subsequent analyses.

Movies were obtained for five DNA samples with 2.69- to 48.5-kbp lengths. For lengths less than about 24 kbp, jump dynamics are similar to those shown in Fig. 2. Molecules smaller than 2 kbp are difficult to identify against the background, whereas those larger than 24 kbp behave differently. The entropic barriers transport mechanism accounts for the jump dynamics observed across the 2.69- to 24-kbp range and corresponds to the 0.14- to 0.52-μm macromolecular radii of gyration (*20*). These radii are greater than the hole radius, and with the radius of gyration recognized as a small measure of coil size, the molecules can be viewed as squeezing through the holes. According to the entropic barriers transport mechanism (*9*, *10*), molecular configurations spanning two cavities define a transition state possessing a higher free energy than that of a chain occupying a single cavity. The higher free energy corresponds to a reduced number of configurations (i.e.,

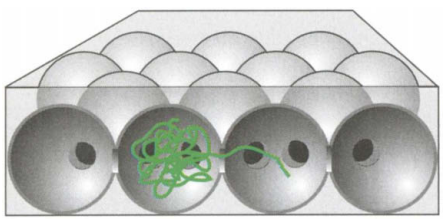

Fig. 1. Schematic of a DNA molecule trapped inside the cavity array.

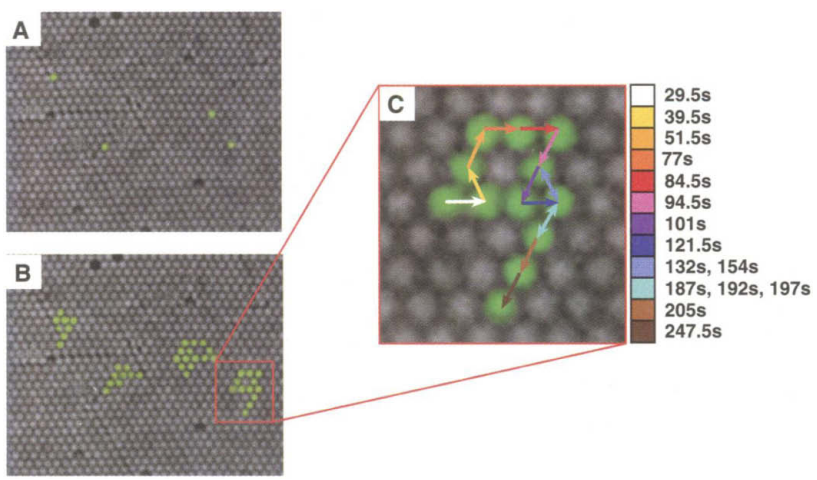

Fig. 2. Visualization of 7.25-kbp DNA trajectories. (**A**) Still frame displaying four DNA molecules trapped inside single cavities. (**B**) Overlay of 500 consecutive frames of the same molecules. (**C**) Expanded image of the path taken by one molecule. The color code provides the times along this path at which the molecule jumped between cavities.

a lower configurational entropy) for a flexible chain "pinched" along its length.

Ideally, a molecule equilibrated inside a single cavity should jump randomly in time and direction to one of six neighboring cavities. Such uncorrelated jumps follow Poisson time statistics (*21*), an expectation checked by plotting histograms of $P(n)$, the probability that n jumps are taken in time interval τ. With τ adjusted to equalize approximately the average number of jumps, Fig. 3 compares measured histograms to Poisson distributions. Excellent agreement is found between measured and predicted values of $P(n)$. A single parameter, the average jumping frequency Γ, characterizes a Poisson distribution. As molecular size grows from 2.69 to 24 kbp, Γ decreases from 0.187 to 0.017 s^{-1}, corresponding to an average interval between jumps of several seconds to several tens of seconds. As expected, larger molecules move more sluggishly.

Einstein (*22*, *23*) first derived the relation between the diffusion coefficient D and random molecular displacements of average magnitude a. Extrapolated to two dimensions, his theory predicts:

$$D = \frac{a^2\Gamma}{4}$$

Equating a to the cavity diameter and substituting Γ measured for 4.36-kbp DNA, this formula predicts that D equals 2.45 × 10^{-10} cm^2/s, representing the microscopic prediction of D. After a large number of jumps, he showed that the mean-square-position displacement $\langle r^2 \rangle$ depends linearly on time t, where in two dimensions:

$$D = \frac{1}{4}\frac{d\langle r^2 \rangle}{dt}$$

For 4.36-kbp DNA, Fig. 4A plots $\log\langle r^2 \rangle$ versus $\log t$ and, as expected, data are well fit by a line of slope equal to unity. The line's intercept reveals that D equals 2.3 × 10^{-10} cm^2/s, representing the macroscopic prediction of D. The microscopic and macroscopic values for D are essentially identical. In the absence of confinement, D for the same DNA is 1.94 × 10^{-8} cm^2/s, approximately two orders of magnitude larger than in the array (*20*). Confinement produces both hydrodynamic and configurational interactions that reduce D, but hydrodynamic interactions play a much smaller role (*2*, *24*).

Visualizations of molecular motion, combined with Poisson jump statistics, verify the dominance of entropic barriers transport for the sizes less than 24 kbp. These statistics also provide D as a function of M, as plotted in Fig. 4B. The data in the figure reasonably conform to scaling theories (*9*, *15*) for entropic barriers transport that argue for an approximately exponential dependence of D on M. The constrained diffusion literature more frequently correlates this dependence through a power law, $D \propto M^{-\nu}$. Forcing the power-law form, a satisfactory fit is obtained with $\nu = 1.1 \pm 0.07$. In typical diffusion studies (i.e., those without visualizations), a ν value so close to unity would be interpreted as evidence for nearly unconstrained (Rouse) diffusion of freely drained DNA molecules (*24*). Visualizations unambiguously demonstrate the error of this interpretation. The ability of different functions to correlate D reflects the limited span of M and freedom in choice of fitting parameters. Only through visualization can the correct diffusion mechanism in the arrays be identified. A quantitative assessment of D trends in terms of theories for constrained diffusion will be published elsewhere.

Unexpectedly, histograms of jump direction are not fully in accord with random jumping, because molecules exit cavities preferentially in the forward direction (i.e., through the hole opposite to the one by which they entered) and also in the backward direction (i.e., through the same hole by which they entered). The forward bias weakens as time spent in a cavity increases. This time dependence suggests that some molecules jump before becoming fully equilibrated and that partial memory of the deformation undertaken to enter a cavity forward biases the direction of exiting. The backward bias, on the other hand, seems independent of time spent in a cavity. This bias is believed to manifest hole polydispersity; DNA molecules are expected to jump more frequently backward and forward between cavities bridged by a larger than average hole. To investigate the possibility, the hole diameter distribution was determined by freeze-fracture scanning electron microscopy, and an SD of 40 nm was found. Such breadth is consistent with the measured backward bias. Because both biases of jump direction are small, neglecting

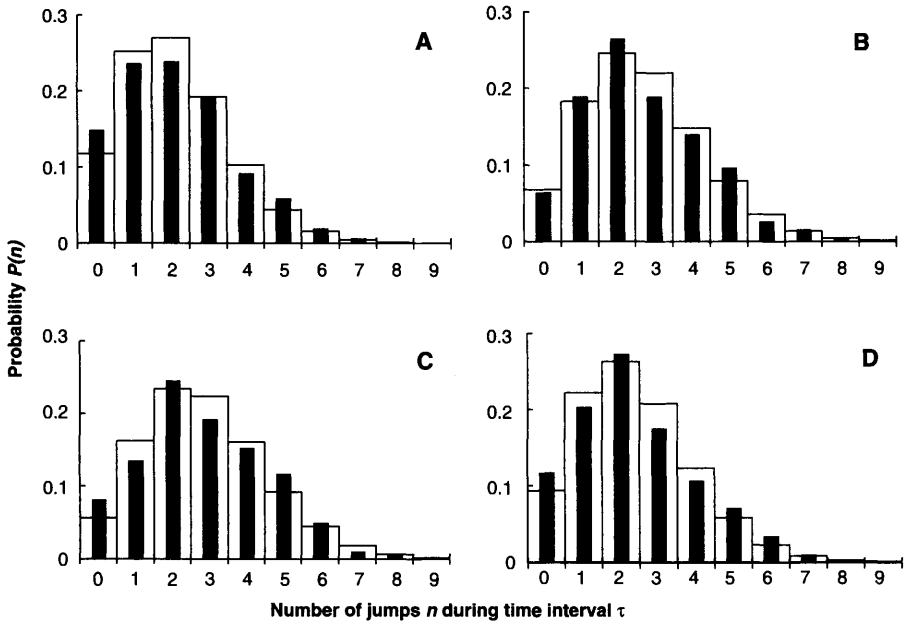

Fig. 3. Measured values of $P(n)$ (plotted as black bars) compared to Poisson distributions (plotted as white bars) with identical means. (**A**) 24.3 kbp (R_g = 0.52 μm), τ = 125 s, Γ = 0.017 s^{-1}. (**B**) 7.25 kbp (R_g = 0.26 μm), τ = 50s, Γ = 0.053 s^{-1}. (**C**) 4.36 kbp (R_g = 0.18 μm), τ = 25 s, Γ = 0.115 s^{-1}. (**D**) 2.69 kbp (R_g = 0.14 μm), τ = 12.5 s, Γ = 0.187 s^{-1}.

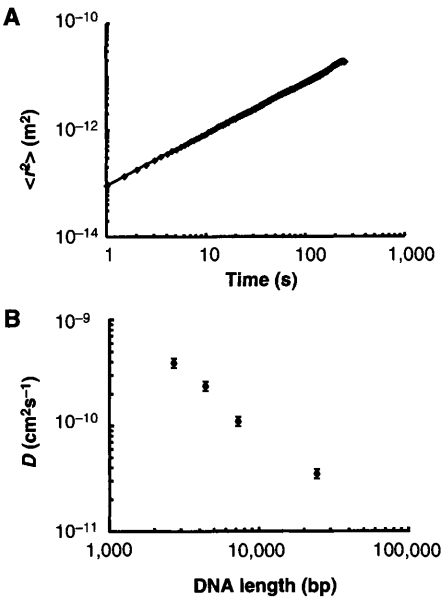

Fig. 4. DNA diffusion analysis. (**A**) The linearity of the mean square displacement as a function of time for 4.36-kbp DNA reveals diffusive transport, with the molecule's diffusion coefficient given by the intercept. (**B**) Variation of diffusion coefficient with molecular weight when the observed mode of diffusion is jumping from cavity to cavity.

directional bias in the diffusion analysis is inconsequential.

Figure 5 displays a series of unequally timed images of 48.5-kbp DNA, the largest of this study. The equilibrium radius of gyration and contour length are 0.73 and 22 μm, respectively (*20*). Fully stretched, this molecule would span more than 20 cavities, seemingly enough to define a reptation tube. Indeed, some aspects of reptation are noted in this molecule's motion. Nevertheless, as indicated in Movie S2 (SOM), most aspects of the motion differ markedly from classic reptation. With a fluctuating number of cavities occupied, motion is more akin to the bunching and stretching of an inchworm. In contrast to the smaller DNA molecules, diffusion can no longer be interpreted in terms of discrete cavity-to-cavity jumps. Although localization to a single cavity still occurs, the dominant configuration is occupation of two adjacent cavities. Figure 5 shows a variety of three- and four-cavity configurations that are both bent and straight. Interestingly, linear molecules spanning three or four cavities rarely form new configurations through "hernias" that spill out laterally from central cavities. Instead, the molecules dominantly alter configuration by expanding or contracting from the cavities that appear to host end segments. The persistence length of DNA is about 50 nm, so hernias would be expected to form readily in the interconnecting holes (*25*). We tentatively ascribe the dynamics for this largest DNA to the beginnings of a crossover from entropic barriers transport to reptation.

Macromolecular diffusion in constrained environments has important technological and scientific ramifications. Most macromolecular separation techniques rely on the selective penetration and/or diffusion of macromolecules within gels and other media of ill-defined pore structure. In this context, switching from disordered to patterned media promises to improve both speed and resolution (*26–29*). Success as a separation medium hinges on the proper choice of pattern chemistry, feature size, dielectric mismatch, and surface charge. Weighed against its most prominent competitor, lithography, one can identify several advantages for colloidal templating—broad choice of pattern chemistry, reduced dielectric mismatch, and straightforward elimination of surface charge. On the other hand, the number of pattern geometries possible through colloidal templating remains limited (*30*).

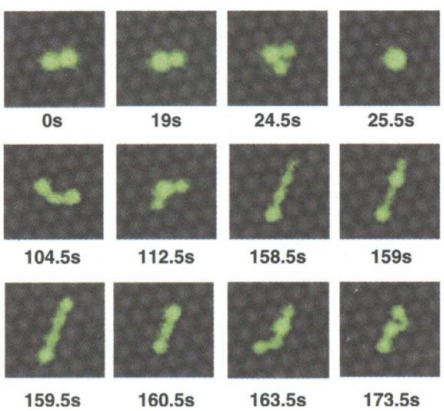

Fig. 5. A sampling at various times of configurations observed for a single 48.5-kbp DNA. The diffusing molecule has been recentered in each image.

References and Notes

1. T. W. Houseal, C. Bustamante, R. F. Stump, M. F. Maestre, *Biophys. J.* **56**, 507 (1989).
2. M. Matsumoto *et al.*, *J. Polym. Sci. B Polym. Phys.* **30**, 779 (1992).
3. J. Käs, H. Strey, E. Sackmann, *Nature* **368**, 226 (1994).
4. T. T. Perkins, D. E. Smith, S. Chu, *Science* **264**, 819 (1994).
5. D. L. Smisek, D. A. Hoagland, *Science* **248**, 1221 (1990).
6. G. W. Slater, P. Mayer, G. Drouin, *Methods Enzymol.* **270**, 272 (1996).
7. A. G. Ogston, *Trans. Faraday Soc.* **54**, 1754 (1958).
8. S. W. Turner, M. Cabodi, H. G. Craighead, *Phys. Rev. Lett.* **88**, 128103 (2002).
9. M. Muthukumar, A. Baumgärtner, *Macromolecules* **22**, 1937 (1989).
10. ———, *Macromolecules* **22**, 1941 (1989).
11. B. H. Zimm, O. Lumpkin, *Macromolecules* **26**, 226 (1993).
12. P. G. de Gennes, *J. Chem. Phys.* **55**, 572 (1971).
13. M. Doi, S. F. Edwards, *J. Chem. Soc. Faraday Trans. II* **74**, 1789 (1978).
14. T. P. Lodge, N. A. Rotstein, S. Prager, *Adv. Chem. Phys.* **79**, 1 (1990).
15. G. Guillot, L. Léger, F. Rondelez, *Macromolecules* **18**, 2531 (1985).
16. L. Masaro, X. X. Zhu, *Prog. Polym. Sci.* **24**, 731 (1999).
17. S. H. Park, Y. Xia, *Chem. Mater.* **10**, 1745 (1998).
18. P. Jiang, K. S. Hwang, D. M. Mittleman, J. F. Bertone, V. L. Colvin, *J. Am. Chem. Soc.* **121**, 11630 (1999).
19. L. Liu, P. Li, S. A. Asher, *Nature* **397**, 141 (1999).
20. D. E. Smith, T. T. Perkins, S. Chu, *Macromolecules* **29**, 1372 (1996).
21. J. W. Haus, K. W. Kehr, *Phys. Rep.* **150**, 263 (1987).
22. A. Einstein, *Ann. Phys.* **17**, 549 (1905).
23. ———, *Z. Electrochem. Angew. Phys. Chem.* **14**, 235 (1908).
24. P.-G. de Gennes, *Scaling Concepts in Polymer Physics* (Cornell Univ. Press, Ithaca, NY, 1979), pp. 193–197.
25. B. Åkerman, *Phys. Rev. E* **54**, 6686 (1996).
26. W. D. Volkmuth, R. H. Austin, *Nature* **358**, 600 (1992).
27. J. Han, S. W. Turner, H. G. Craighead, *Phys. Rev. Lett.* **83**, 1688 (1999).
28. C.-F. Chou *et al.*, *Proc. Natl. Acad. Sci. U.S.A.* **96**, 13762 (1999).
29. L. Meistermann, B. Tinland, *Phys. Rev. E* **52**, 4014 (2000).
30. K. P. Velikov, C. G. Christova, R. P. A. Dullens, A. v. Blaaderen, *Science* **296**, 106 (2002).
31. Support from the University of Massachusetts Material Research Science and Engineering Center. Engaging discussions of diffusion with M. Muthukumar are also acknowledged.

Supporting Online Material

www.sciencemag.org/cgi/content/full/297/5583/987/DC1

Movies S1 and S2

25 April 2002; accepted 5 July 2002

Formation of Immiscible Alloy Powders with Egg-Type Microstructure

C. P. Wang, X. J. Liu, I. Ohnuma, R. Kainuma,* K. Ishida

The egg-type core microstructure where one alloy encases another has previously been obtained during experiments in space. Working with copper-iron base alloys prepared by conventional gas atomization, we were able to obtain this microstructure under gravity conditions. The minor liquid phase always formed the core of the egg, and it sometimes also formed a shell layer. The origin of the formation of this core microstructure can be explained by Marangoni motion on the basis of the temperature dependence of the interfacial energy, which shows that this type of powder can be formed even if the cooling rate is very high.

Alloys immiscible in the liquid-phase region are characterized by a layer structure similar to that of the observed separation between oil and water, and thus they have been considered to be of no use for technical applications (*1*). Much effort has thus been made to obtain a finely dispersed distribution of both liquid phases (*2–5*). One of the most interesting trials was an experiment in space under microgravity conditions (*3*, *4*). For Al-In alloys, instead of a uniformly dispersed structure, an unexpected core microstructure was observed consisting of two layers with the Al-rich phase at the core of the sample (*3*). This fact suggests that it is difficult to obtain a finely dispersed microstructure, even without the influence of gravity.

In the present study, hypermonotectic Cu-Fe base alloys, in which the difference of density (ρ_{Fe} = 6.7 g/cm^3 and ρ_{Cu} = 7.5

Department of Materials Science, Graduate School of Engineering, Tohoku University, Aoba-yama 02, Sendai 980-8579, Japan.

*To whom correspondence should be addressed. E-mail: kainuma@material.tohoku.ac.jp